
Article:
Campbell, R. orcid.org/0000-0001-7114-9863, Davis, M. F., Fazakerley, M. et al. (1 more author) (2015) Taming Tin(IV) Polyazides. Chemistry - A European Journal, 21 (51). pp. 18690-18698. ISSN 0947-6539

https://doi.org/10.1002/chem.201503478

Taming Tin(IV) Polyazides

Rory Campbell, Martin F. Davis, Mathew Fazakerley and Peter Portius*[a]

The first charge neutral Lewis base adducts of tin(IV) tetraazide, $Sn(N_3)_4(bpy)$, $Sn(N_3)_4(phen)$ and $Sn(N_3)_4(py)_2$ and the salt bis{bis(triphenylphosphine)iminium} hexa(azido)stannate $(PPN)_2Sn(N_3)_6$ have been prepared using covalent or ionic azide transfer reagents and ligand exchange reactions. The azides were isolated on the 0.3 to 1 g scale and characterized by infrared and nuclear magnetic resonance spectroscopies, microanalytical and thermal methods and their molecular structures determined by single crystal X-ray diffraction methods. All complexes have a *pseudo*-octahedral $Sn[N]_6$ coordination geometry and possess greater thermal stability than their Si and Ge homologs. The nitrogen content of the adducts of up to 44% exceed any Sn(IV) compound known hitherto.

Introduction

p-Block elements form neutral, binary azides of the type $E(N_3)_n$, n = 1-4.[1,2] The known compounds of this type in group 14 are the tetraazides of carbon[3] and silicon[4] as well as lead[5] and the recently reported tin diazide.[6] Endothermicity, stability and sensitivity of azides are primarily determined by the degree of covalence of the E–N bonds and the nitrogen content. In group 14, $C(N_3)_4$ leads in these criteria having the highest N-content and the most covalent E–N bonds, rendering it extremely sensitive to external stimuli that cause apparently unprovoked explosive decomposition. As a consequence, $C(N_3)_4$ in particular, and also its heavier homologs cannot be isolated by conventional methods. In contrast, our previous work demonstrated that the related complex ions $E(N_3)_6^{2-}$ [4,8,9] and neutral $E(N_3)_4(L_2)$, E = Si,[4] Ge,[9] L_2 = bpy, phen, possess significantly increased stability (T_{dec} up to ~250 °C) and reduced sensitivity which allowed their isolation and full characterization. The increased stability in these coordination compounds arises from the combined effects of lower specific endothermicities due to reduced nitrogen content, and changes in the nature of the E–N bonds caused by hyper-coordination which raises the activation barriers for N_2 elimination. It has been proven previously[1] that these stable, negatively charged complex hexa(azido) ions as well as the charge-neutral adducts of binary azides with nitrogen heterocycles can be synthesized by reactions of NaN_3 with suitable chlorides, followed by either salt metathesis or ligand exchange. This methodology opens up an exciting route to the thus far elusive $E(N_3)_4(L_2)$ polyazido complexes of the heavier homolog, tin, which may lead to much sought-after sufficiently insensitive, lead-free, nitrogen-rich energetic materials.

Ionic azido group transfer reagents, in particular NaN_3, have been employed in the syntheses of many covalent main group element azides including the first known tin azides, $R_3Sn\text{-}N_3$, R = Ph,[10] Me.[11] In these syntheses, the net gain in lattice energy between NaN_3 and NaCl plays a decisive role. Other versatile approaches use hydrazoic acid[12] or azidotrimethylsilane, $TMS\text{-}N_3$, as covalent transfer reagents in reactions with hydrides and fluorides, respectively. The latter method has the great advantage of both $TMS\text{-}N_3$ and the by-product TMS-F being volatile, which greatly assists the isolation of the target polyazides, especially at low temperature. The driving force for the azide group transfer reaction involving $TMS\text{-}N_3$ and fluorides arises primarily from the unusually high dissociation energy of covalent Si–F bonds.[1a,c,d] Similar to organic azides, tin azides undergo N_2 elimination reactions with phosphines to yield phosphinimines, and cycloaddition reactions with alkynes and nitriles to afford triazoles and tetrazoles,[13] which so far precluded preparation / isolation of charge-neutral, nitrogen-rich tin compounds such as $Sn(N_3)_4$. Whilst tin polyazides of the type $Sn(N_3)_6^{2-}$,[14–25] $SnMe_2(N_3)_4^{2-}$,[26] $SnF_m(N_3)_n^{2-}$, $m + n = 6$,[27] $SnCl_2(N_3)_2$,[28] $SnCl_4(N_3)_2^{2-}$ [29] have been known for some time, charge-neutral, nitrogen-rich tin complexes including $Sn(N_3)_4$ have not been reported. Early insight into the structure and bonding in poly(azido)stannate(IV) complexes was based on vibrational,[15-17] Mössbauer,[19,20] ^{14}N NMR,[21] and ^{119}Sn NMR[30] spectroscopies. Herein we describe the first successful synthesis, isolation and characterization of diverse neutral tetra(azido)tin(IV) complexes bearing mono or bidentate pyridine-based ancillary ligands. Analytical and crystallographic results provide direct insight into the structure and bonding in this class of compounds.

Results and Discussion

Syntheses

The reactions involved in the synthesis of the title compounds are outlined in Scheme 1. Disodium hexa(azido)stannate, $Na_2Sn(N_3)_6$ (**1**), was prepared by modification of the method reported by Wiberg *et al.*,[14] from $SnCl_4$ and NaN_3 using acetonitrile (MeCN) as reaction solvent. The less reactive nature of $SnCl_4$ (compared to $SiCl_4$[8] and $GeCl_4$[9]) necessitates a sequential conversion using two batches of NaN_3, each in excessive molar ratio, and longer reaction times (24 h) in order to drive the Cl / N_3 exchange to completion. The procedure afforded stock solutions

[a] Department of Chemistry
The University of Sheffield
Brook Hill, S11 9DR, U.K.
E-mail: p.portius@sheffield.ac.uk
https://www.sheffield.ac.uk/chemistry/staff/profiles/peter_portius

Supporting information for this article is given via a link at the end of the document.

of compound **1**, which can be stored indefinitely (> 6 months) at −30ºC in the dark, and used for the syntheses of compounds **2**, **3** and **5** (*vide infra*). Intriguingly, while the silicon and germanium complexes of the type $E(N_3)_4(L_2)$, E = Si, Ge, L_2 = 2,2'-bipyridine (bpy), 1,10-phenanthroline (phen) are synthesized readily by reaction of $Na_2E(N_3)_6$ solutions and the N-heterocyclic ligand,[4,9] the solutions of **1** do not react with either bidentate ligand, hence no changes are observable in the spectral regions of either asymmetric ($\nu_{as}(N_3)$) or symmetric azide stretching vibrations ($\nu_s(N_3)$) in the *in-situ* FTIR spectra. The volatile components of the stock solution of **1** were evaporated to leave a white powder, the reactivity of which was tested using alternative solvents. IR spectroscopy data show that addition of a polar coordinating solvent (THF) merely re-dissolves the $Na_2Sn(N_3)_6$ and ligand (bpy or phen) mixture.

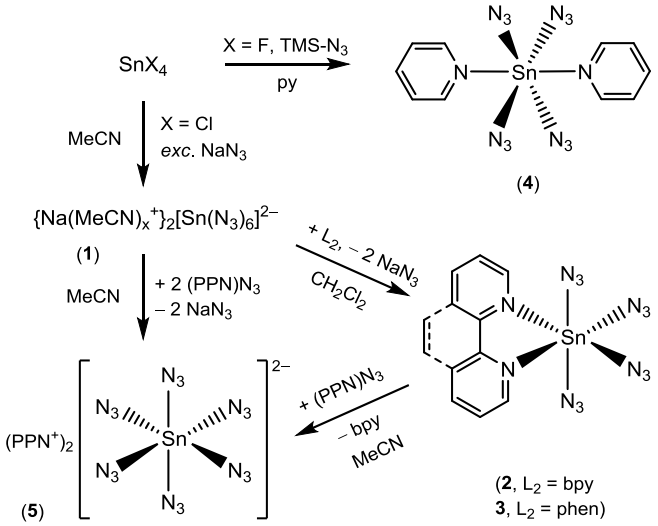

Scheme 1 Synthesis of the poly(azido)tin complexes **2-5**, py: pyridine, bpy: 2,2'-bipyridine; phen: 1,10-phenanthroline, PPN: $N(PPh_3)_2$, TMS: $SiMe_3$.

However, upon addition to **1** of the relatively polar, non-coordinating solvent CH_2Cl_2, in which **1** is insoluble, new bands at 2112 and 2084 cm^{-1} due to $\nu_{as}(N_3)$ stretches, as well as shifts in the characteristic vibrations of bpy or phen in the fingerprint region, 1200 – 1700 cm^{-1}, were observed in the IR spectrum of CH_2Cl_2 extract, indicating the formation of new polyazido species which are soluble in CH_2Cl_2. The new polyazido tin compounds $Sn(N_3)_4(L_2)$, L_2 = bpy (**2**) or phen (**3**) were isolated as analytically pure, white, slightly air sensitive solids upon filtration of the CH_2Cl_2 reaction mixtures and extraction of the NaN_3-containing solid residues, followed by evaporation of the combined extraction solutions and recrystallization from MeCN. Both compounds are only sparingly soluble in MeCN, THF and CH_2Cl_2. An investigation into the reactivity of **1** with pyridine (py) showed the route involving direct N_3 / py ligand exchange to be impractical. Addition of an excess of pyridine to a MeCN solution of **1** caused the precipitation of NaN_3 as evidenced by the appearance of the characteristic IR bands. After removal of the MeCN under vacuum, extraction of the turbid viscous mixture with warm CH_2Cl_2 afforded a small amount of a new tin azide. Alternatively, extraction of the mixture with pyridine carried through a small proportion of NaN_3 impurity, from which it is difficult to separate the reaction product owing to their similarly low solubility in most solvents. Thus it must be concluded from these results that even though tin(IV) chloride forms complexes with pyridine of the type *trans*-$SnCl_4(py)_2$ as has been demonstrated previously,[45] the related per(azido) complex *trans*-$Sn(N_3)_4(py)_2$ (**4**) is inaccessible using NaN_3 as an azido group transfer reagent. However, TMS-N_3 reacts slowly at r.t. with a solution of SnF_4 in pyridine. Spectroscopic monitoring of this reaction shows the continuous intensity decrease of the $\nu_{as}(N_3)$ band of TMS-N_3 at 2137 cm^{-1} and the growth of new IR absorption bands at lower frequencies. At a reaction temperature of 45 °C and allowing for overpressure relieve, this process is complete after 16 hours. The new azido compound can be separated from the reaction mixture by evaporation of the volatile components which results in a white raw-product. Analytically pure **4** can be obtained by recrystallization from a warm mixture of pyridine / MeCN. Compound **4** is insoluble in CH_2Cl_2 and THF, only sparingly soluble in MeCN and pyridine, and insoluble in hydrocarbons. As expected, sodium hexa(azido)stannate (**1**) reacts readily with $(PPN)N_3$ upon precipitation of NaN_3. The cation exchanged hexa(azido)stannate salt (**5**) can be obtained from the supernatant solution straight-forwardly as colorless crystals.

Spectral properties

The IR spectra of the complexes **2** and **3** are characterized by prominent absorption bands at 2081-2112 cm^{-1} which are assigned to $\nu_{as}(N_3)$ stretches of azido groups (N_3 groups). The considerably higher energies of these stretching vibrations in comparison to that of the N_3-anion (*ca*. 2000 cm^{-1})[44] indicates the coordinated nature of the N_3-groups in these species. Both complexes thus fit well into the series of the related $E(N_3)_4(L_2)$ and $E(N_3)_6^{2-}$ species as heavier group 14 homologs. However,

Table 1. Selected frequencies (cm^{-1}) of characteristic IR absorption bands of compounds **2**-**5** in MeCN solution The data for analogous silicon (**2-Si**, **3-Si**, **5-Si**) and germanium complexes (**2-Ge**, **3-Ge**, **5-Ge**) are shown for comparison.

Compound	$\nu_{as}(N_3)$ [a]	$\nu_s(N_3)$ [b]	$\nu(L)$ [c]
$Sn(N_3)_4(bpy)$ (**2**)	2111, 2081	1337, 1282	1615, 1603
$Ge(N_3)_4(bpy)$ (**2-Ge**) [d]	2120, 2097, 2091	1288 [e]	1621, 1607
$Si(N_3)_4(bpy)$ (**2-Si**) [f]	2151, 2126, 2116	1316	1623, 1615
$Sn(N_3)_4(phen)$ (**3**)	2112, 2085	1331, 1279	1525
$Ge(N_3)_4(phen)$ (**3-Ge**) [d]	2120, 2093	1286	1523
$Si(N_3)_4(phen)$ (**3-Si**) [f]	2150, 2126, 2118	1315	1583
$Sn(N_3)_4(py)_2$ (**4**)	2111, 2083	1335, 1285	1612
$(PPN)_2Sn(N_3)_6$ (**5**)	2079 [g]	1338, 1289	-
$(PPN)_2Ge(N_3)_6$ (**5-Ge**) [d]	2083	1297	-
$(PPN)_2Si(N_3)_6$ (**5-Si**) [h]	2109	1316	-

[a] asymmetric N_3 stretch; [b] symmetric N_3 stretch; [c] characteristic ring breathing mode, L = py, bpy or phen, respectively; [d] ref. (9); [e] CH_2Cl_2 solution; [f] see ref. (4); [g] a second, weak band is observed at 2112 cm^{-1}; [h] see ref. (8).

the $\nu_{as}(N_3)$ frequencies in **2** and **3** are lower by approximately 30-40 cm^{-1} than those observed in $Si(N_3)_4(bpy)$ (**2-Si**) and $Si(N_3)_4(phen)$ (**3-Si**), and by 10 cm^{-1} than $Ge(N_3)_4(bpy)$ (**2-Ge**) and $Ge(N_3)_4(phen)$ (**3-Ge**). Unlike the Si / Ge analogs, there is little difference in $\nu_{as}(N_3)$ between the bpy and phen Sn complexes (Table 1). Furthermore, while theory predicts that OC-6-12 symmetric $E(N_3)_4(L_2)$ complexes with non-linear N_3 coordination should give rise to four IR-active $\nu_{as}(N_3)$ stretches, only two bands are observed in the spectra of **2** and **3**. This discrepancy is interpreted in terms of band overlap. Similar observations were made previously for Si and Ge complexes where only two (**2-Ge**, **3-Ge**) or three (**2-Si**, **3-Si**) $\nu_{as}(N_3)$ bands can be discerned. Complex **4** exhibits two IR active $\nu_{as}(N_3)$ stretches which rules out a C_{4h} symmetry of the $Sn(N_3)_4$ fragment and rather suggests an out-of-plane, S_4 symmetric arrangement of N_3 ligands. The NMR spectral data (Table 2) in **2** and **3** are in accord with the postulated OC-6-12 symmetry. According to the chemical shift difference $\Delta\delta_{DA} = \delta(H_D) - \delta(H_A)$, where H_D denotes the protons most sensitive to ligands (N_3, F-Br) and coordination centers (Si-Sn) in positions 6,6' (bpy) and 2,9 (phen), the strength of the electron withdrawing effect of the N_3 ligands lies in between those of F and Cl ligands. The polarizing effect leads to a deshielding of H_D that decreases relative to H_A in the series of bpy complexes Si > Ge > Sn. This effect is somewhat weaker in the related phen complexes. Both NMR and IR spectral data support the notion that in the studied solutions the complexes **2** and **3** exist in un-dissociated form, whereas **4** is insufficiently soluble to allow solution NMR studies.

Table 2. ^1H NMR chemical shifts [ppm] [a] for **2** and **3**, showing silicon, germanium, fluoro, chloro and bromo analogues for comparison.

Complex	$\delta(H_A)$	$\delta(H_B)$	$\delta(H_C)$	$\delta(H_D)$	$\Delta\delta_{DA}$	
$Sn(N_3)_4(bpy)$, **2**	8.08	8.55	8.72	9.12	1.04	[b]
$Ge(N_3)_4(bpy)$, **2-Ge**	8.06	8.52	8.81	9.35	1.29	[c]
$Si(N_3)_4(bpy)$, **2-Si**	8.00	8.48	8.63	9.40	1.40	[d]
$SnF_4(bpy)$	8.49	8.99	9.15	9.41	0.92	[e]
$SnCl_4(bpy)$	8.38	8.84	9.35	9.66	1.28	[f]
$SnBr_4(bpy)$	8.46	8.87	9.39	9.81	1.35	[f]
$Sn(N_3)_4(phen)$, **3**	8.34	8.39	9.09	9.42	1.08	[b]
$Ge(N_3)_4(phen)$, **3-Ge**	8.34	8.41	9.08	9.59	1.25	[c]

$Si(N_3)_4$(phen), **3-Si**	8.28	8.38	9.03	9.60	1.32	[d]
SnF_4(phen)	8.45	8.45	9.16	9.35	0.90	[g]

[a] H_A, H_B, H_C and H_D refer to $H_{5,5'}$, $H_{4,4'}$, $H_{3,3'}$, $H_{6,6'}$ of bpy, and $H_{3,8}$, $H_{4,7}$, $H_{5,6}$, $H_{2,9}$ of phen, respectively; $\Delta\delta_{DA} = \delta_{DA} - \delta_{DA}$; [b] MeCN-$d_3$; [c] THF-$d_8$, ref. (9), this paper; [d] MeCN-d_3, ref. (4); [e] $MeNO_2$-d_3, ref. (31); [f] *N,N*-dimethyl-acetamide, ref. (32); [g] CH_3Cl-d, ref. (31).

Reactivity

Both $Sn(N_3)_4$(bpy) (**2**) and $Sn(N_3)_4$(phen) (**3**) are white crystalline solids which hydrolyze slowly in air, whereas $Sn(N_3)_4(py)_2$ (**4**) remains stable in air for days. **2** and **3** are moderately soluble in CH_2Cl_2 and MeCN, and insoluble in hydrocarbons, but **4** is insoluble in aprotic solvents and reacts with dimethyl sulfoxide by displacement of pyridine as shown by IR and NMR spectra (see figures S17 and S28). **2-4** have good thermal stability and appear to be insensitive to impact and friction. Compound **2** reacts with $(PPN)N_3$ in MeCN solution by displacement of bpy. This reaction was monitored at ambient temperature by *in situ* IR spectroscopy which shows the conversion of **2** (2081, 2111 cm^{-1}) into $[Sn(N_3)_6]^{2-}$ (2079, 2112 cm^{-1}) (**5**) and uncoordinated bpy (1584 cm^{-1}) within 2 h (Scheme 1, Fig. 1).

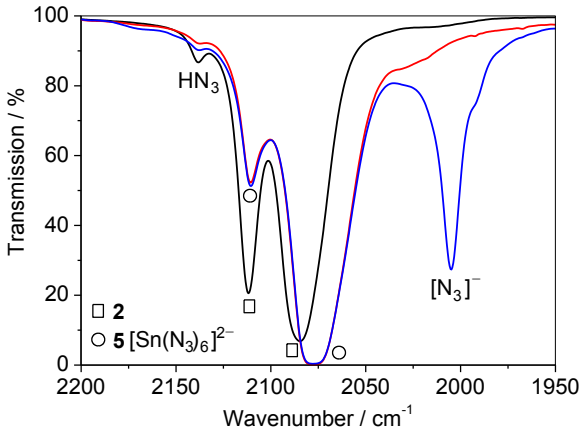

Fig. 1 In-situ FTIR spectra of the reaction of $Sn(N_3)_4$(bpy) (**2**) with $(PPN)N_3$ in MeCN: black (**2**); red, 2 h after addition of two molar equivalents of $(PPN)N_3$; blue, followed by addition of further $(PPN)N_3$; 2005 cm^{-1}; HN_3, 2138 cm^{-1}; (**2**), 2085 cm^{-1} and 2112 cm^{-1} (**$Sn(N_3)_6^{2-}$**), 2079 cm^{-1} 2112 cm^{-1} (N_3^-).

The thermal behavior of the tin polyazides was investigated by differential scanning calorimetry (DSC) measurements according to which the onset of exothermic decomposition occurred at temperatures ranging from 265 – 305 °C, which are higher than those of the lighter homologs (Table 3). To the best of our knowledge, complex **4** has the highest onset temperature, T_{on}^{dec} = 305 °C, of any group 14 polyazide (including $Pb(N_3)_2$). All calorigrams exhibit large decomposition exotherms (for example for compound **5** see Fig. 2) from which the molar heats of decomposition, ΔH_{dec} (MJ mol^{-1}), of –0.89, –0.93, –1.10 and –0.77 were derived for the compounds **2**, **3**, **4** and **5**, respectively. While the specific enthalpies for these compounds are less negative in comparison to their lighter homologs (Fig. 2 inset), the accuracy of measurements (< ±10%) does not allow for an evaluation of molar enthalpic differences between homologs which must arise from variations in bond energies. However, the available data on the Si, Ge and Sn compounds reveals a strong correlation (R^2 = 0.98) between the nitrogen content n(N) × 14.01 / M_r (Fig. 2, inset) and the specific enthalpy of decomposition. Assuming a linear relationship implies an enthalpic contribution of –4.30 (±0.14) kJ g^{-1} (nitrogen). Similarly, each N_3 ligand contributes on average –208(±7) kJ mol^{-1} to the molar enthalpy of decomposition per formula unit. Using –4.30 kJ g^{-1}, the specific enthalpies of decomposition of the Sn compounds can be predicted to be ΔH_{dec} / (kJ g^{-1}) = –1.91(±6) (**2**), –1.81(±6) (**3**), –1.90(±6) (**4**), –0.83(±3) (**5**).

Table 3. Comparison of thermal properties of compounds **2**, **3**, **4** and **5** with the lighter group 14 homologs.[a]

Compound	T_{on}^{m} / °C	T_{on}^{dec} / °C	ΔH_{dec} / (kJ g^{-1})	
$Sn(N_3)_4$(bpy), **2**	180	265	–2.00	this work

$Ge(N_3)_4(bpy)$, **2-Ge**	190	252	–2.13	ref. (8) [b]
$Si(N_3)_4(bpy)$, **2-Si**	212	265	–2.42	ref. (4)
$Sn(N_3)_4(phen)$, **3**	200	301	–2.00	this work
$Ge(N_3)_4(phen)$, **3-Ge**	192	251, 303	–1.39 [d]	ref. (8) [b,c]
$Si(N_3)_4(phen)$, **3-Si**	216	239	–2.29	ref. (4) [c]
$Sn(N_3)_4(py)_2$, **4**	265	305	–1.74	this work
$(PPN)_2Sn(N_3)_6$, **5**	218	300, 365	–0.76	this work
$(PPN)_2Ge(N_3)_6$, **5-Ge**	194	256, 312	–0.85	ref. (8)
$(PPN)_2Si(N_3)_6$, **5-Si**	214	256, 321	–0.92	ref. (7)

[a] T_{on}^{m}, onset temperature of melting; T_{on}^{dec}, onset temperature(s) of decomposition; ΔH_{dec} enthalpy of decomposition as determined from the integrated area under the exotherm [calibration detailed in experimental section]; [b] see SI: [c] MeCN hemisolvate; [d] upper limit.

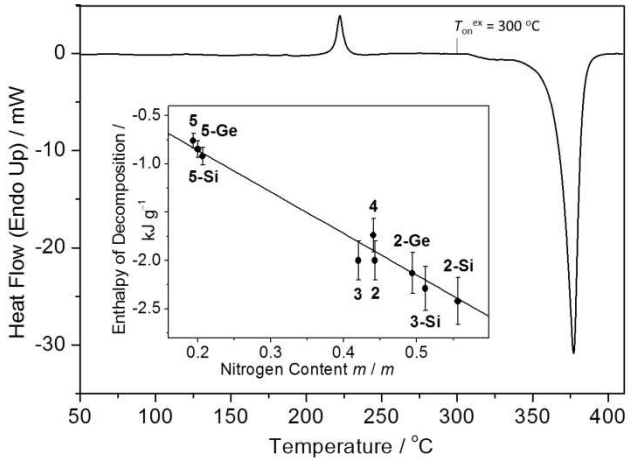

Fig. 2. Differential scanning calorimetry trace of $(PPN)_2Sn(N_3)_6$ (**5**) showing melting at T_m = 218 °C and a two-step exothermic decomposition which begins at T_{dec} = 300°C; inset: Correlation between nitrogen content and decomposition enthalpy of diverse Si, Ge and Sn polyazides.

X-ray Crystallography

Crystals suitable for single crystal X-ray diffraction measurements were obtained from MeCN solutions by cooling their respective saturated solutions slowly to –20°C overnight (**2, 3**, **5**)

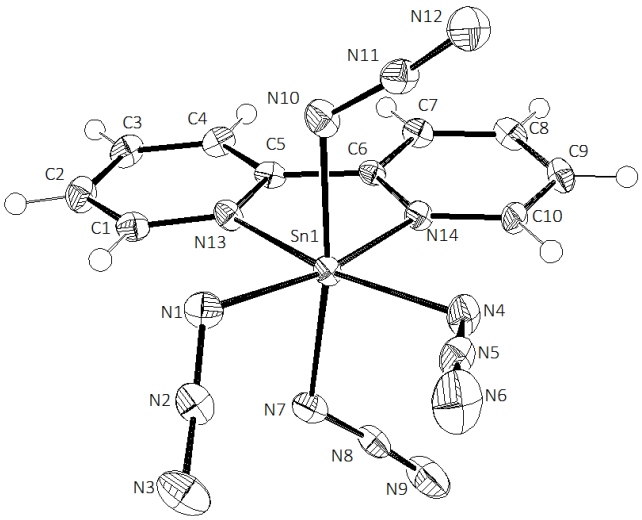

Figure 2. ORTEP drawing showing the molecular structure of compound **2** at 120 K with the thermal ellipsoids at the 50% probability level. Selected bond lengths [Å] and angles [°]: Sn1-N1 2.097(6), Sn1-N4 2.110(5), Sn1-N7 2.101(6), Sn1-N10 2.101(6), Sn1-N13 2.204(6), Sn1-N14 2.211(5), N1-N2 1.214(8), N2-N3 1.144(8), N4-N5 1.204(9), N5-N6 1.150(10), N7-N8 1.203(8), N8-N9 1.136(9), N10-N11 1.228(8), N11-N12 1.126(8), N13-Sn1-N14 74.3(2), N1-Sn1-N4 102.6(2).

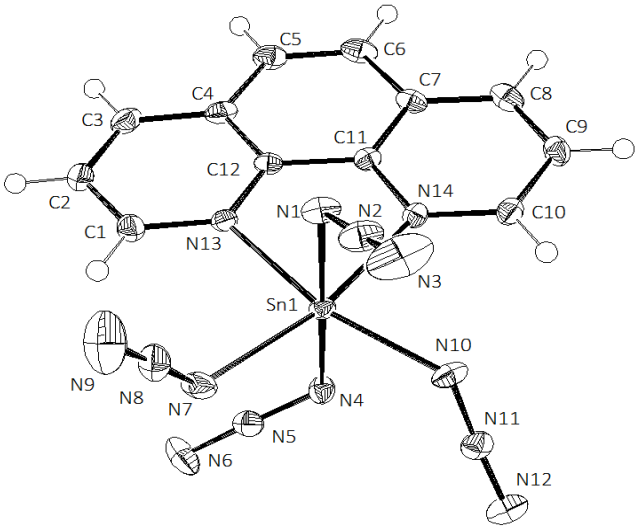

Figure 3. ORTEP drawing showing the molecular structure of compound **3** at 100 K with the thermal ellipsoids at the 50% probability level. Selected bond lengths [Å] and angles [°]: Sn1-N1 2.109(2), Sn1-N4 2.113(2), Sn1-N7 2.118(2), Sn1-N10 2.090(2), Sn1-N13 2.225(2), Sn1-N14 2.228(2), N1-N2 1.218(3), N2-N3 1.141(3), N4-N5 1.216(3), N5-N6 1.144(3), N7-N8 1.213(3), N8-N9 1.144(3), N10-N11 1.222(3), N11-N12 1.142(3), N13-Sn1-N14 74.56(7), N7-Sn1-N10 104.11(9).

or by slow cooling of a hot (~65°C) solution in a MeCN-pyridine mixture to ambient temperature (**4**). The structure solution resulted in accurate molecular structures for all four data sets (Table 5). Supplementary crystallographic data for this paper can be obtained free of charge from the Cambridge Crystallographic Data Centre *via* www.ccdc.cam.ac.uk/data_request/cif (CCDC 1039722 (**2**), 1039723 (**3**), 1062323 (**4**), 1039721 (**5**) and the SI). Table 4 gives a summary of key molecular structure parameters with a comparison to those of Si and Ge analogues determined previously. The tetraazides as well as the hexa(azido)stannate anion have more (**2**, **3**) or less (**4**, **5**) distorted octahedral Sn[N]$_6$ coordination frameworks. Whereas the molecular structures of **2**, **3** and **5** resemble those of the lighter E(N$_3$)$_4$(L$_2$) and [E(N$_3$)$_6$]$^{2-}$ homologs, complex **4** adopts an all-*trans* OC-6-11 geometry with all four azido ligands (N$_3$ ligands) in the equatorial plane while both co-planar pyridine ligands are found in the axial positions with the tin occupying a crystallographic inversion centre. The structural influence of the investigated pyridine-based ligands onto N$_3$ ligands of the tin complexes appears to be minimal. This notion is evident, for instance, from the minimal and maximal *d*(Sn-N$_\alpha$) and ΔNN parameters given in Table 4 as well as other valence angles and bond lengths, which are all very similar or indistinguishable within the accuracy of the measurement. For instance, in the chelate complexes **2** and **3**,

Table 4. Crystallographically determined bonding parameters of Group 14 poly(azido) complexes.

Compound	*d*(E-N$_\alpha$) / Å	ΔNN$_{av}$ / pm [a]	N-E-N / ° [b]
Si(N$_3$)$_4$(bpy) [c]	1.818(2), 1.864(2)	6.5(4), 8.6(4)	81, 97
Si(N$_3$)$_4$(phen) [c]	1.828(1), 1.860(1)	7.2(4), 8.4(3)	82, 98
Si(N$_3$)$_6^{2-}$ [d]	1.866(1), 1.881(1)	5.4(4), 6.0(4)	-
Ge(N$_3$)$_4$(bpy) [e]	1.925(2), 1.972(2)	6.6(5), 8.6(6)	79, 99
Ge(N$_3$)$_4$(phen) [f]	1.939(2), 1.963(2)	7.9(4), 9.0(4)	80, 100
Ge(N$_3$)$_6^{2-}$ [e]	1.969(2), 1.980(2)	6.1(7), 7.1(6)	-
Sn(N$_3$)$_4$(bpy) **2** [g]	2.100(6), 2.116(6)	5.8(19), 9.9(16)	74, 103
Sn(N$_3$)$_4$(phen) **3** [g]	2.090(2), 2.118(2)	6.4(5), 8.0(4)	75, 105
Sn(N$_3$)$_4$(py)$_2$ **4**	2.105(2), 2.120(2)	6.8(6), 8.7(6)	-
Sn(N$_3$)$_6^{2-}$ **5** [g]	2.122(2), 2.147(2)	5.9(6), 9.5(11)	-

[a] average over the independent distances $\Delta NN = \Sigma_{i=1}^{n} [d(N_\alpha\text{-}N_\beta)_i - d(N_\beta\text{-}N_\gamma)_i] / n$ (estimated standard deviation); [b] $N_L\text{-}E\text{-}N_L$ bite angle; $N_\alpha\text{-}E\text{-}N_\alpha$ (*cis*) inter azido ligand angle in the plane of the bidentate ligand; [c] ref. (4) and SI; [d] ref. (8); [e] ref. (9); [f] CCDC 1415857, see SI; [g] this paper.

no significant differences in bond lengths can be found between equatorial and axial N_3 ligands as Sn–N_α bond lengths are spread out over a range where Sn–N_α(ax) lie in between those of Sn–N_α(eq) bonds, and *cis* and *trans* positions are indistinguishable within the same narrow range 2.097(6)-2.110(5) Å and 2.090(2)-2.118(2) Å, respectively. Furthermore, the *trans* influence of azide and pyridine-based ligands on N_3 ligands in the tin complexes are indistinguishable crystallographically (Sn-N_α(cis) in **2** and **3**, 2.09-2.12 Å; Sn-N_α (trans) in **4**, 2.11 Å, 2.12 Å). Being a poorer σ-electron donor, Sn–N bonds to phenanthroline are somewhat longer, by 1.5(6) pm than those to bipyridine. The same observation can be made for Si and Ge complexes: 1.3(2) pm (Si), 1.4(2) pm (Ge). The substitution of all four chloro ligands for N_3 ligands in the tetrachloro analogues $SnCl_4$(bpy) 2.236(6) Å,[33] and $SnCl_4$(phen) 2.237(3) Å,[34] leads to a shortening of the Sn–N(L_2) bonds by about 2 pm and this reveals the weaker σ-electron donor capabilities of N_3 ligands which is in line with conclusions drawn from the NMR data (*vide supra*).[46]

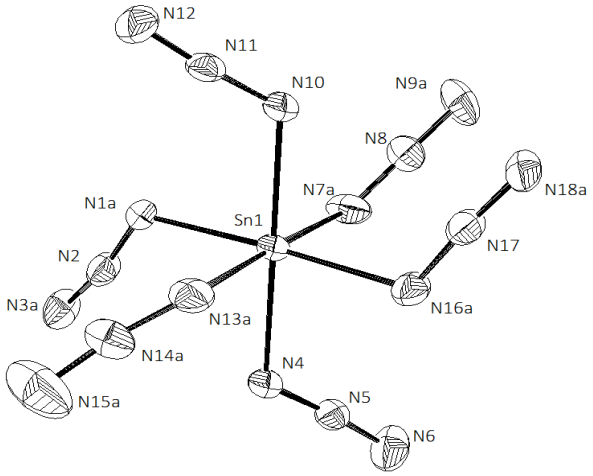

Figure 4. ORTEP drawing showing one part of the disordered $[Sn(N_3)_6]^{2-}$ anion in the crystal of **5** at 100 K with the thermal ellipsoids at the 50% probability level. Selected bond lengths [Å] and angles [°]: Sn1-N1a 2.131(3), Sn1-N4 2.1222(17), Sn1-N7a 2.146(3), Sn1-N10 2.1220(18), Sn1-N13a 2.147(3), Sn1-N16a 2.133(3), N1a-N2 1.207(4), N2-N3a 1.142(4), N4-N5 1.210(3), N5-N6 1.148(3), N7a-N8 1.206(4), N8-N9a 1.146(4), N10-N11 1.212(3), N11-N12 1.143(3), N13a-N14a 1.222(10), N14a-N15a 1.128(6), N16a-N17 1.213(4), N17-N18a 1.146(4). N1a-Sn1-N16a 178.7(3), N4-Sn1-N10 177.84(7), N7a-Sn1-N13a 177.9(3), Sn1-N1a-N2 120.2(3), N1a-N2-N3a 176.4(9), Sn1-N7a-N8 122.3(3), N9a-N8-N7a 174.0(13), Sn1-N13a-N14a 118.6(17), N13a-N14a-N15a 170.0(30), Sn1-N16a-N17 119.3(3), N18a-N17-N16a 175.5(16).

With the Sn–N_α bonds of the neutral mixed-ligand polyazides **2** to **4** falling within the 2.090(2) to 2.120(2) Å length range, it is the homoleptic, negatively charged hexa(azido)stannate **5** that has significantly longer bonds 2.122(2)-2.147(3) Å. Hence, it is the complex charge which has the greatest influence on the Sn-N_α distance leading to a lengthening by 2 to 3 pm. The charge effect is of the same extent in the analogous Si and Ge systems. The relative orientation of the four N_3 groups appears to be governed by numerous, weak intermolecular C–H···(N_3-ligand) interactions (d / Å = 2.3, **2**; 2.4, **3**; 2.7, **4**; 2.5, **5**) at the level of van der Waals contacts (d_{vdW}(NH) = 2.7 Å) as well as intramolecular N_α, N_β dipole-dipole interactions as short as 3.0 Å (**2** and **5**), 2.9 Å (**3** and **4**) (d_{vdW}(NN) = 3.2 Å).[35] The increasing E-N(L_2) distances for the tin complexes necessitate narrower bite angles than where E = Si, Ge. Intriguingly, the Sn complexes adopt a geometry in between octahedral (90°) and trigonal bipyramidal (120°) with the equatorial N_3 groups that oppose the bidentate ligand now sharing angles of 103° and 105°, whereas the axial N_3 ligands are closer to the required positions and share angles of 170° (**2**) and 176° (**3**), respectively. The molecular structure of the hexa(azido)stannate anion has been reported previously[22] in the $(PPh_4)_2Sn(N_3)_6$ salt which adopts triclinic *P*–1 crystal symmetry in which the tin atom occupies a special position with inversion symmetry that renders only three N_3 groups crystallographically independent. The reflections for this structure determination were measured at room temperature,[22] whereas crystals of compounds **2**-**5** were studied at low temperature. The hexa(azido)stannate $(PPN)_2Sn(N_3)_6$ (**5**) also crystallizes in *P*–1; however, tin occupies a general position resulting in six crystallographically unique N_3 groups of which four are disordered. Figure 4 shows a thermal ellipsoid plot of $Sn(N_3)_6^{2-}$ in **5** obtained from the structure solution and refinement with the disordered components omitted for clarity. Any Cl / N_3 ligand substitutional disorder in the crystal of **5** was confirmed absent by elemental analysis. Therefore, the comparably large thermal ellipsoids for several ligating N atoms found in initial structure solutions are attributed to a concerted wagging vibration about the N_β–Sn–N_β' axes. The weak interionic interactions between the non-coordinating PPN^+ and the $Sn(N_3)_6^{2-}$ species are presumed to allow for this flexibility around an approximate S_6 geometry. A disorder model was adopted to account for this thermal motion in which either N_α and N_γ or all atoms for an azide group were split into two half-occupied positions. Suitable restraints within the *Shelxtl* software were applied during the

refinement such that the two disordered components had similar geometry (SADI, SIMU, DELU commands). Further refinement details, and all crystallographic data are included in the supporting information.

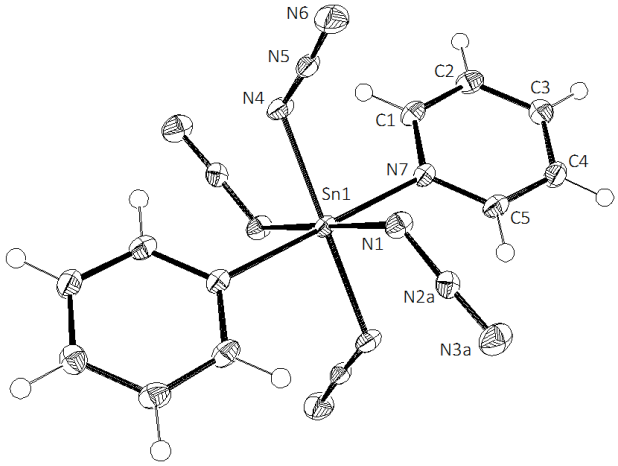

Figure 5. ORTEP drawing showing the complex *trans*-$Sn(N_3)_4(py)_2$ in the crystal of **4** at 100 K with thermal ellipsoids at the 50% probability level. One component of the disordered azide group is omitted for clarity. Selected bond lengths [Å] and angles [°]: Sn1-N1 2.1051(15), Sn1-N4 2.1195(16), Sn1-N7 2.2262(16), N1-N2a 1.221(3), N2a-N3a 1.142(3), N4-N5 1.218(2), N5-N6 1.140(2), N1-Sn1-N7 90.95(6), N4-Sn1-N7 89.80(6).

Conclusions

The first neutral adducts of tin tetraazide, and a new hexa(azido)stannate(2–) salt have been prepared by salt metathesis or salt elimination reactions involving chelating pyridine ligands and the versatile disodium intermediate (**1**). The reaction of tin(IV) fluoride with azidotrimethylsilane has demonstrated to be a highly effective alternative route to covalent tin azides such as **4**. The tin polyazides have been isolated and fully characterized. Their spectral and thermal behavior follows general trends that are governed by nitrogen contents and overall charges on complexes as well as size and electronegativity of the coordination centre. In the crystal, all complexes have distorted octahedral $Sn[N]_6$ coordination with N_3 ligands that often adopt disordered orientations. The neutral Lewis base adducts of $Sn(N_3)_4$ show slightly higher thermal stability than the related adducts of $Si(N_3)_4$ and $Ge(N_3)_4$, but lower sensitivity toward atmospheric moisture than the stabilized hexa(azido)silicate(IV) salt $(PPN)_2Sn(N_3)_6$ in solution. A new method has been developed to access and isolate charge-neutral polyazido tin complexes which extends the concept of Lewis base stabilization to monodentate ligands. The new findings lay the foundations for the coordination of a great diversity of N-rich ancillary ligands and open up routes to related compounds in Group 14 and, potentially, a replacement for lead azide.

Experimental Section

All experiments were carried out under an atmosphere of argon using Schlenk tube or glovebox techniques. CAUTION: appropriate safety precautions should be taken when working with tin azides. Compound **1** was isolated only in a small quantity (<<100 mg) for the purpose of recording a FTIR spectra in the solid state. MeCN (Fisher, 99.9 %), MeCN-d_3 (Aldrich, 99.8 %) and CH_2Cl_2 (Sigma Aldrich, >99.8 %) were dried over CaH_2 (Acros, 93 %) for 18 h, and trap-to-trap condensed. 2,2'-bipyridine and 1,10-phenanthroline (both Acros, 99 %) were sublimed prior to use. $SnCl_4$ (Aldrich, 99 %) was stirred over anhydrous Na_2CO_3 for 18 h and trap-to-trap condensed. NaN_3 (Acros, >99 %) was dried under vacuum (*ca.* $4x10^{-2}$ mbar) at 120 °C overnight. $(PPN)N_3$ was prepared according to a literature procedure,[36] recrystallized from MeCN, and then dried under vacuum (*ca.* $4x10^{-2}$ mbar) overnight at 120 °C. Infrared absorption spectra were recorded in the range 500-4000 cm^{-1} on a Bruker Tensor 27 Fourier transform infrared (FTIR) spectrometer running the Bruker *OPUS* software package, or Bruker Alpha FTIR spectrometer running *OPUS 7.0*, at a spectral resolution of 2 cm^{-1}, either as a nujol mull between NaCl windows or in solution using a Specac CaF_2 solution cell. The relative absorbance of bands in FTIR spectra are indicated by the abbreviations vs (very strong), s (strong), m (medium), w (weak), vw (very weak), sh (shoulder) and br (broad). Elemental analyses were carried out by the University of Sheffield elemental analysis service on a PerkinElmer 2400 CHNS/O series II elemental analyser in an atmosphere of pure O_2. ^1H and ^{13}C Nuclear magnetic resonance (NMR) spectra were recorded using a 400 MHz Bruker Avance 400 spectrometer; ^{31}P spectra were recorded on a 250 MHz Bruker Avance 250 spectrometer. ^1H and ^{13}C NMR spectra were calibrated against the residual solvent peak according to ref. [37]. DSC calorigrams were recorded on a PerkinElmer Pyris 1 Differential Scanning Calorimeter operated under N_2 flow (20 ml min^{-1}) with a heating rate of 10°C min^{-1}. The instrument was calibrated against pure In as reference (99.999 %) (T_{trans} = 156.60 °C, ΔH = 28.45 J g^{-1}). The samples were sealed in stainless steel high-pressure capsules (internal volume 30 µL, Au-plated Cu seals, rated up to 400 °C, 150 bar, Perkin Elmer). Onset temperatures (T_{on}), mass losses (Δm), enthalpies of fusion (ΔH_{fus}), and decomposition (ΔH_{dec}) were calculated using the data analysis tools

within the Pyris 1 software. Baseline correction was applied to DSC traces using Microcal *Origin 6.0*, by fitting a suitable polynomial over the temperature range. X-ray diffraction (XRD) data collection was performed at 100 K (unless otherwise specified) on a Bruker SMART 4000 or Kappa diffractometer with CCD area detector. All data were collected using graphite-monochromated Mo $K_{\alpha 1,2}$ radiation (λ = 0.71073 Å). Data was collected using Bruker *APEX2* software[38] and integrated using Bruker *SAINT*,[39] absorption correction was applied using *SADABS*. Structures **2**, **3**, and **5** were solved with *SHELXS-97* using direct methods for the location of heavy atoms, whereas **4** was solved by intrinsic phasing using *SHELXT*[41] within *APEX2*. Hydrogen atom positions were calculated and all structures were refined using the *SHELXTL-2013* software suite.[42] H atom positions were determined geometrically. Thermal ellipsoid plots of the crystal structures were produced using *ORTEP-3 for Windows*.[43]

Disodium hexa(azido)stannate, $\{Na(MeCN)_x\}_2Sn(N_3)_6$ (1): (adapted from ref. [14]) $SnCl_4$ (0.15 ml, ρ = 2.2 g cm^{-3}, 1.3 mmol) was added to a vigorously stirred suspension of NaN_3 (0.787 g, 12.1 mmol) in MeCN (20 ml) at 0 °C. The suspension was allowed to warm to r.t., and was left to stir for 24 h before filtration onto a second batch of NaN_3 (522 mg, 8.03 mmol). The resultant white suspension was left to stir for a further 24 h before filtration, and the white filter residue was extracted with MeCN (2 × 15 ml) yielding a perfectly clear, colorless solution of (**1**). An approximate concentration was calculated based on complete conversion of $SnCl_4$ and the mass of the solution (ρ(MeCN) = 0.786 g cm^{-3}). The stock solution concentration typically ranged from 0.05 - 0.3 mol dm^{-3} depending on the amount of $SnCl_4$ (1.3 - 2.6 mmol) and MeCN used. IR (Nujol, cm^{-1}) $\tilde{\nu}$ = 3374vw,br, 3340vw, 2118vs, 2090sh, 2077vs, 1660w, 1349m, 1298m, 1293sh, 1247vw; MeCN: 2112w, 2078vs, 1339w, 1289w.

Tetra(azido)(2,2'-bipyridine)tin (2): Dry, sublimed bipyridine (378 mg, 2.42 mmol) was added to an aliquot of a stock solution of **1** (11.0 ml, ~1.6 mmol) in MeCN. The MeCN was removed in vacuo behind a blast shield, then CH_2Cl_2 (60 ml) was added. The stirred reaction mixture was heated to 40 °C for 2 h yielding a white suspension. The suspension was filtered and the residue extracted with a further 80 ml of boiling CH_2Cl_2. The combined filtrate and extract solutions were concentrated to a volume of 4 ml and then cooled to −28 °C for 1 h upon which crystallization occurred. The supernatant solution was decanted, the residue extracted with MeCN (80 ml) at 60 °C and the solution then concentrated to 2 ml and cooled to −28 °C overnight which caused recrystallization. The cold mother liquid was decanted, the residue washed with MeCN (1 ml) and dried in vacuo at 60 °C for 2 h, giving **2** (477 mg, 1.08 mmol) as a white powder in 67 % yield based on **1**. Elem. anal. (%) for $C_{10}H_8N_{14}Sn$, 442.93 g mol^{-1}, calcd: C 27.12, H 1.82, N 44.26; found: C 27.72, H 1.86, N 42.91. IR (nujol, cm^{-1}) $\tilde{\nu}$ = 3441vw, 3356m, 3334m, 3122vw, 3116vw, 3082w, 3065vw, 3040vw, 3033vw, 2110vs, 2092vs,br, 2075vs,br, 2067vs,br, 1612w, 1600w, 1573w, 1565w, 1497w, 1477w, 1445m, 1332m, 1318w, 1277w, 1273w, 1228vw, 1252w, 1176w, 1160w, 1108vw, 1073vw, 1061 vw, 1046vw, 1033m, 1023w, 776 m, 767w, 663vw, 651vw, 589vw; MeCN: 2111m, 2081vs, 1615w, 1604 w, 1333vw, 1321sh, 1282w; CH_2Cl_2: 2112m, 2084vs, 1614w, 1602w, 1332vw, 1321w. NMR (MeCN-d_3) δ(^{1}H) / ppm = 8.08 (ddd, 2*H*, H5,5'), 8.55 (ddd, 2*H*, H4,4'), 8.72 (ddd, 2*H*, H3,3'), 9.12 (ddd, 2*H*, H6,6'); coupling constants [Hz]: ^3J(H3,H4) = 8.0, ^4J(H3, H5) = 1.1, ^5J(H3,H6) = 1.0, ^3J(H4,H5) = 7.7, ^4J(H4,H6) = 1.6, ^3J(H5,H6) = 5.5; δ(^{13}C) = 125.5, 130.1, 144.6, 145.9, 147.5. DSC: melting T_{on} = 180 °C; decomposition 265 °C, ΔH_{dec} = −880 kJ mol^{-1} (−2.00 kJ g^{-1}).

Tetra(azido)(1,10-phenanthroline)tin (3): Dry, sublimed phenanthroline (242 mg, 1.34 mmol) was added to an aliquot of a stock solution of **1** (25.9 ml, ~1.3 mmol) in MeCN. The procedure for isolating the compound was carried out as for **2** (*vide supra*), except the crude **3** was extracted with 15 ml of MeCN at 40 °C. White crystals of **3** (270 mg, 0.578 mmol) were obtained after recrystallization from MeCN in 44 % yield based on **1**. Elem. anal. (%) for $C_{12}H_8N_{14}Sn$, 466.95 g mol^{-1}, calcd: C 30.87, H 1.73, N 41.98; found: C 31.07, H 1.45, N 41.92. DSC: melting T_{on} = 200 °C; decomposition T_{on} = 301 °C, ΔH_{dec} = 934 kJ mol^{-1} (−2.00 kJ g^{-1}). IR (Nujol, cm^{-1}) $\tilde{\nu}$ = 2114s, 2096s, 2082s, 2068s, 1628vw, 1621w, 1610w, 1587 w, 1581w, 1573w, 1548w, 1519w, 1332m, 1275m, 1225w, 1147w, 1108w, 976w, 849w, 779 w, 717s, 653s, 594m; MeCN = 2112, 2086, 1630w, 1612w, 1589vw, 1526sh; CH_2Cl_2: 2112m, 2085vs, 1630w, 1611w, 1588 vw, 1525sh. NMR (MeCN-d_3) δ(^{1}H) / ppm = 8.34 (dd, 2*H*, H3,H8), 8.39 (s, 2*H*, H5,H6), 9.09 (dd, 2*H*, H4,H7), 9.42 (dd, 2*H*, H2,H9); coupling constants [Hz]: ^3J(H2,H3) = ^3J(H8,H9) = 5.1, ^4J(H2,H4) = ^4J(H7,H9) = 1.4, ^3J(H3,H4) = ^3J(H7,H8) = 8.3; δ (^{13}C) / ppm = 127.7, 129.2, 131.2, 135.0, 144.7, 148.3.

Tetra(azido)bis(pyridine)tin (4): SnF_4 (292 mg, 1.50 mmol) was suspended in pyridine (20 ml), and TMS-N_3 (710 mg, 6.16 mmol) was added dropwise to the suspension over ~1 minute under vigorous stirring. The Schlenk tube containing the off-white reaction mixture was fitted with a Hg stop valve, immersed in an oil bath set to 45 °C, and the mixture stirred for 16 h during which time TMS-F (b.p. 15 °C) was driven off. The tube was then allowed to cool to r.t. The supernatant liquid was decanted leaving 303 mg of white powder. This residue was suspended in MeCN (25 ml) and warmed to 55 °C before as much pyridine was added dropwise until all material had dissolved. Slow cooling of this hot saturated solution to ambient temperature afforded colourless block crystals, from which the solvent was decanted, and the crystals dried in vacuo for 2 h. Yield 270 mg (40 % based on **1**). Elem. anal. (%) for $C_{10}H_8N_{14}Sn$, 444.99 g mol^{-1}, calcd: C 26.99, H 2.27, N 44.06; found: C 27.15, H 2.04, N 43.70. DSC: melting T_{on} = 265 °C; decomposition T_{on} = 305 °C, ΔH_{dec} = −775 ± 10 kJ mol^{-1} (−1.74 ± 0.02 MJ kg^{-1}). IR (cm^{-1}): nujol $\tilde{\nu}$ = 3405vw, 3347w, 3114vw, 3104vw, 3076vw, 3054vw, 3034vw, 2600w, 2545vw, 2500vw, 2494vw, 2103sh, 2085vs, 1662vw, 1609m, 1571w, 1540vw, 1483s, 1450 vs, 1393vw, 1356vw, 1332s, 1280s, 1250 vw, 1209m, 1188vw, 1182vw, 1162m, 1144vw, 1094vw, 1063s, 1044s, 1015s, 1009vw, 877m, 782vw, 772vw, 760s, 705vw, 692s, 657m, 644s, 592m; pyridine: 2109m, 2081vs, 1610vw, 1560vw, 1540vw, 1488w, 1451 m, 1334m, 1283m, 1257m, 1084 vw, 1046vw; MeCN: 2111m, 2083vs, 1612vw, 1335w, 1285m; CH_2Cl_2: 2107w, 2089s,1613vw, 1327w. No reliable solution NMR data could be obtained due to the poor solubility of compound **4**.

Bis{bis(triphenylphosphine)iminium} hexa(azido)stannate (5): (PPN) N_3 (1.100 g, 1.89 mmol) was dissolved in an aliquot (15 ml, 0.95 mmol) of the MeCN stock solution of **1** and the resultant mixture stirred for 0.5 h yielding a fine, white suspension. In order to dissolve all soluble material, further MeCN (35 ml) was added to the stirred suspension until no further dissolution was noticeable. The suspension was then filtered yielding an absolutely clear, colourless solution and an off-white residue which was discarded. The volume of the solution was reduced until crystallisation commenced. Crystallization was completed by storing in the freezer overnight. The white, crystalline precipitate was isolated by decantation of the solvent, washing with MeCN at −35 °C and then drying in *vacuo* at ambient temperature for 3 h, giving 967 mg (0.668 mmol) of $(PPN)_2Sn(N_3)_6$ in 70 % yield with respect to **1**. Elem. anal. (%) for $C_{72}H_{60}N_{20}P_4Sn$, 1447.99 g mol^{-1}, calcd: C 59.72, H 4.18, N 19.35; found: C 59.71, H 4.03, N 19.41. DSC melting T_{on} = 218 °C, decomposition T_{on} = 365 °C, ΔH_{dec} = −0.76 kJ g^{-1}. IR (Nujol, cm^{-1}) $\tilde{\nu}$ = 2104vw,br, 2074vs, 2060m,sh, 1438w, 1337w, 1316w, 1303w, 1288w, 1269w, 1118w, 693w, 551w, 532w; MeCN: 2111 w, 2078vs; CH_2Cl_2: 2111w, 2078vs; THF: 2108w,br, 2075vs. NMR (250 MHz, CD_3CN) δ (^{1}H) / ppm = 1.94

(MeCN solvent residue), 7.44-7.70 (m); δ (^{13}C) / ppm = 1.32 (m, solvent residual), 118.3 (s, solvent residual), 129.2 (s, *ipso*), 130.4 (m, *ortho*), 133.3 (m, *meta*), 134.7 (s, *para*); δ(^{14}N) / ppm = 135.7 (MeCN-d_3), 218.7 (N_γ), 299.1 (N_α); δ(^{31}P) / ppm = 20.8.

Table 5. Crystal structure refinement parameters for compounds **2–5** [a]

	2	**3**	**4**	**5**
Empirical formula	$C_{10}H_8N_{14}Sn$	$C_{12}H_8N_{14}Sn$	$C_{10}H_{10}N_{14}Sn$	$C_{72}H_{60}N_{20}P_4Sn$
M_r	442.99	467.01	445.01	1447.97
Crystal system	monoclinic	trigonal	triclinic	triclinic
Space group	*C*c	*P*3(1)	*P*-1	*P*-1
a [Å]	11.6427(19)	9.985(5)	7.2058(7)	11.7012(8)
b [Å]	8.3153(13)	9.985(5)	8.1954(8)	12.5721(9)
c [Å]	15.866(2)	14.325(5)	8.4689(7)	24.4651(17)
α [°]	90	90	116.634(6)	94.143(4)
β [°]	96.783(6)	90	94.618(7)	101.080(4)
γ [°]	90	120	109.252(6)	103.058(4)
V [Å^3]	1525.2(4)	1236.9(10)	406.31(7)	3415.3(4)
Z	4	3	1	2
D_{calc} [g cm^{-3}]	1.929	1.881	1.819	1.408
μ [mm^{-1}]	1.706	1.583	1.601	0.527
F (000)	864	684	218	1484
Crystal size [mm x mm x mm]	0.27 × 0.18 × 0.10	0.37 × 0.27 × 0.20	0.17 × 0.06 × 0.06	0.50 × 0.38 × 0.30
Θ range for data collection [°]	2.59, 25.00	2.36, 24.97	2.79, 27.96	1.68, 25.00
Limiting indices *h*; *k*; *l*	-13, 13; 9, -9; -18, 18;	-11, 11; -11, 11; -17, 17	-9, 9; -10, 10; -10, 10	-13, 13; -14, 14; -29, 29
Reflections collected	6895	12903	5861	58063
Independent reflections	2683 (R_{int} = 0.0404)	2761 (R_{int} = 0.0204)	1767 (R_{int} = 0.0283)	11980 (R_{int} = 0.0513)
Completeness to Θ [%]	99.8 (Θ = 25.00°)	100.0 (Θ = 24.97°)	99.0 (Θ = 25.24°)	99.8 (Θ = 25.00°)
Refinement method	[b]	[b]	[b]	[b]
Data / restraints / parameters	2683 / 2 / 226	2761 / 1 / 244	1767 / 38 / 133	11980 / 66 / 959
GoF F^2	1.170	1.120	1.065	1.077
Final *R* indices [$I > 2\sigma(I)$]	0.0294	0.0112	0.0190	0.0283
R indices (all data)	0.0970	0.0282	0.0380	0.0770
Largest diff. peak / hole [e Å^{-3}]	0.840 / -0.983	0.256 / -0.234	0.499 / -0.501	0.510 / -0.724

[a] CCDC numbers *vide supra*, temperature of measurement given in captions of fig.s 2 (**2**), 3 (**3**), 4 (**5**) and 5 (**4**); [b] full-matrix least-squares on F^2

Acknowledgements

The authors thank the EPSRC (EP/E054978/1, and E-Futures Doctoral Training Centre Studentship), and the University of Sheffield for support.

Keywords: azides • hypercoordination • weakly coordinating cations • main group elements • polyazides

1. a) P. Portius and M. Davis, *Coord. Chem. Rev.*, **2013**, *257*, 1011–1025, ref.s cited therein; b) W. P. Fehlhammer and W. Beck, *Z. Anorg. Allg. Chem.* **2013**, *639*, 1053–1082, ref.s cited therein; c) T. M. Klapötke, B. Krumm, M. Scherr, R. Haiges, and K. O. Christe, *Angew. Chem. Intl. Ed.*, **2007**, *46*, 8686–8690; d) R. Haiges, J. A. Boatz, J. M. Williams, K. O. Christe, *Angew. Chem. Intl. Ed.*, **2011**, *50*, 8828-8833.
2. Q. S. Li and H. X. Duan, *J. Phys. Chem. A*, **2005**, *109*, 9089–9094.
3. K. Banert, Y.-H. Joo, T. Rüffer, B. Walfort, and H. Lang, *Angew. Chem. Int. Ed.* **2007**, *46*, 1168–1171.
4. P. Portius, A. C. Filippou, G. Schnakenburg, M. Davis, and K.-D. Wehrstedt, *Angew. Chem. Int. Ed.*, **2010**, *49*, 8013–8016.
5. T. Curtius, *Ber.*, **1891**, *24*, 3345.
6. T. G. Müller, F. Karau, W. Schnick, and F. Kraus, *Angew. Chem. Intl. Ed.*, **2014**, *53*, 13695–13697.
7. see also reviews on homoleptic polyazido complexes of main group elements (ref. 1) and transition metals: W.-K. Seok and T. M. Klapötke, *Bull. Korean Chem. Soc.*, **2010**, *31*, 781–788 and references therein.
8. A. C. Filippou, P. Portius, and G. Schnakenburg, *J. Am. Chem. Soc.*, **2002**, *124*, 12396–12397.
9. A. C. Filippou, P. Portius, D. U. Neumann, and K.-D. Wehrstedt, *Angew. Chem. Int. Ed.*, **2000**, *39*, 4333–4336.
10. J. Thayer and R. West, *Inorg. Chem.*, **1964**, *3*, 406–409.
11. J. Thayer and R. West, *Inorg. Chem.*, **1964**, *3*, 889–893.
12. E. Wiberg and H. Michaud, *Z. Naturforsch. B,* **1954**, *9*, 500.
13. H. C. Kolb, M. G. Finn, K. B. Sharpless, *Angew. Chem. Int. Ed.* **2001**, *40*, 2004–2021
14. E. Wiberg and H. Michaud, *Z. Naturforsch. B*, **1954**, *9*, 500–501.
15. D. Forster and W. Horrocks Jr., *Inorg. Chem.*, **1966**, *5*, 1510–1504.
16. W. Beck, E. Schuierer, P. Pöllmann, and W. P. Fehlhammer, *Z. Naturforsch. B*, **1966**, *21*, 811–812.
17. W. Beck, W. P. Fehlhammer, P. Pöllmann, E. Schuirer, and K. Feldl, *Chem. Ber.*, **1967**, *100*, 2335–2361.
18. F. Petillon, M.-T. Youinou, and J.-E. Guerchais, *Bull. Soc. Chim. Fr.*, **1969**, *12*, 4293.
19. R. H. Herber and H.-S. Cheng, *Inorg. Chem.*, **1969**, *8*, 2145–2148.
20. H.-S. Cheng and R. H. Herber, *Inorg. Chem.*, **1970**, *9*, 1686–1690.
21. W. Beck, W. Becker, K. F. Chew, W. Derbyshire, N. Logan, D. M. Revitt, and D. B. Sowerby, *J. Chem. Soc. Dalt. Trans.*, **1972**, 245–247.
22. D. Fenske, H. Dörner, and K. Dehnicke, *Z. Naturforsch. B*, **1983**, *38*, 1301–1303.
23. A. Vogler, C. Quett, A. Paukner, and H. Kunkely, *J. Am. Chem. Soc.*, **1986**, *108*, 8263–8265.
24. G. Barone, A. Silvestri, G. Ruisi, and G. La Manna, *Chem. Eur. J.*, **2005**, *11*, 6185–6191.
25. J. W. Krogh, G. Barone, and R. Lindh, *Chem. Eur. J.*, **2006**, *12*, 5116–5121.
26. J. Halfpenny, *Acta Crystallogr. - Sect. C Cryst. Struct. Commun.*, **1995**, *51*, 2044–2046.
27. P. A. W. Dean and D. F. Evans, *J. Chem. Soc. A*, **1968**, 1154.
28. N. Wiberg and K. Schmid, *Chem. Ber.*, **1967**, *100*, 748–754.
29. V. B. Busch, J. Pebler, and K. Dehnicke, *Z. Anorg. Allg. Chem.*, **1975**, *416*, 203–210.
30. A. Marshall, PhD Thesis: *Spectroscopic and structural studies of tin complexes*, Durham University, **1982**.
31. M. F. Davis, M. Clarke, W. Levason, G. Reid, and M. Webster, *Eur. J. Inorg. Chem.*, **2006**, 2773-2782
32. G. Matsubayashi and J. Iyoda, *Bull. Chem. Soc. Jpn.*, **1977**, *50*, 3055–3056.
33. V. N. N. Zakharov, A. V. V. Yatsenko, A. L. L. Kamyshnyi, and L. A. A. Aslanov, *Koord. Khim.*, **1991**, *17*, 789–794.
34. Z.-H. Su, B.-B. Zhou, Z.-F. Zhao, and S. W. Ng, *Acta Crystallogr. Sect. E Struct. Rep. Online*, **2007**, *63*, m394–m395.
35. a) S. Alvarez, *Dalt. Trans.*, **2013**, *42*, 8617–8636; b) R. S. Rowland and R. Taylor, *J. Phys. Chem.* **1996**, *100*, 7384–7391.
36. J. Songstad, A. Martinsen, *Acta Chim. Scand.* **1977**, *31*, 645–650
37. G. R. Fulmer, A. J. M. Miller, N. H. Sherden, H. E. Gottlieb, A. Nudelman, B. M. Stoltz, J. E. Bercaw, and K. I. Goldberg, *Organometallics*, **2010**, *29*, 2176–2179
38. *APEX2*, Bruker AXS, Madison, Wisconsin, U.S.A.
39. *SAINT*, Bruker AXS, Madison, Wisconsin, U.S.A.
40. *SADABS*, Bruker AXS, Madison, Wisconsin, U.S.A.
41. *SHELXT*, G. M. Sheldrick, *Acta Crystallogr. A,* **2015**, 71, 3-8
42. *Shelxtl-2013*, G. M. Sheldrick, *Acta Crystallogr. A*, **2008**, 64, 112-122
43. *ORTEP-3 for Windows,* L. Farrugia, *J. Appl. Crystallogr.* **1997**, *30*, 565
44. A. C. Filippou, P. Portius, G. Kociok-Köhn, and V. Albrecht, *J. Chem. Soc. Dalton Trans.* **2000**, 1759–1768.
45. I. R. Beattie, M. Milne, M. Webster, H. E. Blayden, P. Jones, R. C. G. Killean, and J. L. Lawrence, *J. Chem. Soc. A,* **1969**, 482–485.
46. the halo-analogues $SnCl_4(py)_2$ and $SnBr_4(py)_2$ have also been studied but their insolubility hindered crystallization and precluded determination of accurate molecular structures (ref. 44).

Charge-neutral tin(IV) azido complexes with nitrogen contents of up to 44% have been prepared. Spectroscopic, structural and thermal characterization reveals trends in reactivity and bonding.

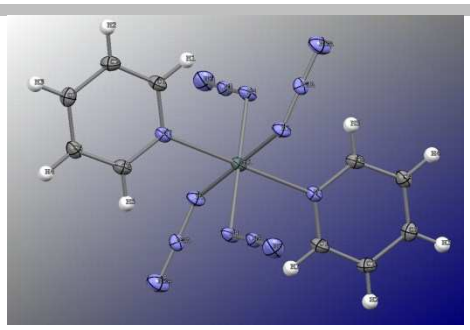

*R. Campbell, M. F. Davis, M. Fazakerley, P. Portius**

Page No. – Page No.

Taming Tin(IV) Polyazides